ARTICLE
Journal of Cellular Biochemistry 115:1937–1947 (2014)

Journal of Cellular Biochemistry

Changes in Chromatin Structure in NIH 3T3 Cells Induced by Valproic Acid and Trichostatin A

Marina Barreto Felisbino,[1] Maria Silvia Viccari Gatti,[2] and Maria Luiza S. Mello[1]*

[1]*Department of Structural and Functional Biology, Institute of Biology, University of Campinas (UNICAMP), 13083-862, Campinas, SP, Brazil*

[2]*Department of Genetics, Evolution and Bioagents, Institute of Biology, University of Campinas (UNICAMP), 13083-862, Campinas, SP, Brazil*

ABSTRACT

Valproic acid (VPA) and trichostatin A (TSA) are known histone deacetylase inhibitors (HDACIs) with epigenetic activity that affect chromatin supra-organization, nuclear architecture, and cellular proliferation, particularly in tumor cells. In this study, chromatin remodeling with effects extending to heterochromatic areas was investigated by image analysis in non-transformed NIH 3T3 cells treated for different periods with different doses of VPA and TSA under conditions that indicated no loss of cell viability. Image analysis revealed chromatin decondensation that affected not only euchromatin but also heterochromatin, concomitant with a decreased activity of histone deacetylases and a general increase in histone H3 acetylation. Heterochromatin protein 1-α (HP1-α), identified immunocytochemically, was depleted from the pericentromeric heterochromatin following exposure to both HDACIs. Drastic changes affecting cell proliferation and micronucleation but not alteration in *CCND2* expression and in ratios of *Bcl-2/Bax* expression and cell death occurred following a 48-h exposure of the NIH 3T3 cells particularly in response to higher doses of VPA. Our results demonstrated that even low doses of VPA (0.05 mM) and TSA (10 ng/ml) treatments for 1 h can affect chromatin structure, including that of the heterochromatin areas, in non-transformed cells. HP1-α depletion, probably related to histone demethylation at H3K9me3, in addition to the effect of VPA and TSA on histone H3 acetylation, is induced on NIH 3T3 cells. Despite these facts, alterations in cell proliferation and micronucleation, possibly depending on mitotic spindle defects, require a longer exposure to higher doses of VPA and TSA. J. Cell. Biochem. 115: 1937–1947, 2014.

KEY WORDS: VALPROIC ACID; TSA; CHROMATIN REMODELING; HETEROCHROMATIN; EPIGENETICS; HP1-α; NIH 3T3 CELLS; *CCND2*; *Bcl-2*; *Bax*

Valproic acid (VPA), a potent anti-convulsant agent, has been reported to inhibit class I histone deacetylases (HDACs) in several cell types when administered in its therapeutic range (0.3–0.7 mM) [Göttlicher et al., 2001; Phiel et al., 2001; Eyal et al., 2004; Kortenhorst et al., 2009]. Class I HDACs are essential for cell proliferation and survival [Dejligbjerg et al., 2008]. Among other known HDAC inhibitors (HDACIs), trichostatin A (TSA) has been identified as a pan-HDACI [Yoshida et al., 1995; Rao et al., 2007].

Considering the effects of VPA and TSA in processes that result in HDAC inhibition, this action is expected to be accompanied by changes in chromatin supra-organization and nuclear architecture. Indeed, it has been found that VPA and TSA induce chromatin decondensation in HeLa cells [Tóth et al., 2004; Rao et al., 2007; Felisbino et al., 2011] and that the treatment of prostate cancer cells with VPA in vitro and in vivo results in dose- and time-dependent changes in nuclear structure [Kortenhorst et al., 2009]. Furthermore, it has been reported that a reduction in cellular proliferation and changes in DNA fragmentation rates are elicited by VPA treatment in HeLa cells [Felisbino et al., 2011]. Previously, an absolute fold-change of 2.29 in cyclin D2 (*CCND2*) gene, but expression with no significant change in caspases and *FAS* genes, had been reported in response to VPA in HeLa cells [Dejligbjerg et al., 2008]. In addition to induced genome-wide histone acetylation, observed in mouse embryonic stem cells [Hezroni et al., 2011], exposure to VPA has also been shown to deplete non-histone proteins that maintain chromatin structure in MCF-7 breast cancer cells, which enhances

The authors declare no potential conflict of interests.

Grant sponsor: FAPESP; Grant numbers: 2010/50015-6, 2009/11763-0; Grant sponsor: CNPq; Grant numbers: 301943/2009-5, 471303/2009-7, 132345/2010-2, 475261/2012-7.

*Correspondence to: Maria Luiza S. Mello, Institute of Biology, University of Campinas, R. Monteiro Lobato 255, 13083-862 Campinas, SP, Brazil. E-mail: mlsmello@unicamp.br

Manuscript Received: 1 November 2013; Manuscript Accepted: 2 June 2014

Accepted manuscript online in Wiley Online Library (wileyonlinelibrary.com): 10 June 2014

DOI 10.1002/jcb.24865 • © 2014 Wiley Periodicals, Inc.

sensitivity of DNA to nucleases and potentiates the activity of DNA-damaging agents [Marchion et al., 2005].

The majority of the effects promoted by VPA have been studied in tumor cells because of the potential chemotherapeutic efficacy of this drug for the treatment of specific types of cancer [Taddei et al., 2005; Duenas-Gonzalez et al., 2008; Gotfryd et al., 2010; Shoji et al., 2012], especially in combination with radiotherapy [Harikrishnan et al., 2008; Shoji et al., 2012], as well as for the treatment of cognitive disorders [Hasan et al., 2013]. Therefore, it appears appropriate investigate the effects of this HDACI and TSA on the chromatin supra-organization of non-tumoral cells such as mouse non-transformed fibroblastic NIH 3T3 cells. The investigation of the higher-order packing states of the chromatin in NIH 3T3 cells under the treatment of HDACIs is particularly interesting because these cells have been extensively used as a model system [Ailenberg and Silverman, 2003; Leibiger et al., 2013] and also because they contain a significant contribution of centromeric heterochromatin in their interphase nuclear phenotype [Mello and Russo, 1990]. If the higher levels of chromatin organization in the heterochromatic bodies of the NIH 3T3 cells were also affected by VPA, image analysis procedures would be effective in detecting this information [Felisbino et al., 2011]. Non-histone proteins of the HP1 (heterochromatin protein 1) family participate in the assembly of macromolecular complexes in chromatin as structural adapters [Taddei et al., 2001]. HP1-α plays a role in the chromatin structure of the chromocenter pericentric heterochromatin in mouse cells [Maison et al., 2002]; therefore, investigating whether this protein is released from the heterochromatin of NIH 3T3 cells as an effect of VPA and/or TSA treatments would illuminate the potential effects of these drugs, besides the effect of inhibition of histone deacetylases, that could be involved with chromatin remodeling and maybe affect cell functions in non-tumoral cells.

Here, we investigated whether VPA and TSA, due to their actions at the epigenetic level, affect chromatin supra-organization, including the presence of HP1-α, in non-transformed fibroblastic NIH 3T3 cells. Chromatin supra-organization, cell death morphology and the evaluation of mitotic indices, chromosome abnormalities and micronuclei were analyzed in Feulgen-stained VPA- and TSA-treated NIH 3T3 cells. The Feulgen image analysis method was chosen because it was previously demonstrated to be a useful assay for studies on chromatin remodeling [Felisbino et al., 2011; Poplineau et al., 2013; Vidal et al., 2014], cell death and mitotic disturbances [Felisbino et al., 2011]. The effects of VPA and TSA on cell survival, HDAC activity and histone H3 acetylation were investigated under the same experimental conditions used for the study of chromatin remodeling to estimate the correlation between these phenomena. In addition, expression analysis was performed for *CCND2* and two genes involved in apoptosis (*Bcl-2* and *Bax*) in VPA-treated cells. Part of this study was communicated at the Epigenetics & Chromatin Conference held at Boston in 2013 [Felisbino et al., 2013].

MATERIALS AND METHODS

CELL CULTURE

NIH 3T3 cells at passage 40 were grown in Dulbecco's modified essential medium (DMEM) (Sigma®, St. Louis) containing 10% fetal calf serum (FCS) (Cultilab®, Campinas, Brazil) and 1% penicillin and streptomycin (Sigma®) (10,000 UI and 100 mg/ml, respectively) and were incubated at 37°C in a 5% CO_2 atmosphere. The cells were originally acquired from the National Institute of Health at passage 7 by Dr. Carmen Verissimo (Institute of Biology, Unicamp, Campinas). The cells were seeded at a concentration of 5×10^4 cells/ml in complete medium for 24 h. Then, they were treated with VPA (Sigma®) dissolved in PBS and diluted in DMEM supplemented with 2% FCS at doses of 0.05, 0.5, and 1.0 mM (1.0 mM = 166.2 μg/ml) for 1, 2, 4, and 24 h. Cells treated with TSA in DMSO (Labsynth, Diadema, Brazil) diluted in DMEM containing 2% FCS (with a final DMSO concentration lower than 1%) at doses of 10, 20 and 100 ng/ml for 1, 2, 4, and 24 h were also used. Untreated cells were used as controls.

CYTOTOXICITY ASSAY

The viability of the NIH 3T3 cells after treatment with VPA and TSA under the experimental conditions used for the study of chromatin supra-organization was assessed using the conventional 3-(4,5-dimethyldiazol-2-yl)-2,5-diphenyl-tetrazolium bromide (MTT) assay (Sigma®) [Denizot and Lang, 1986]. All assays were performed in triplicate. Cell viability after each treatment was expressed relative to the viability of the untreated cells.

CELL FIXATION AND DNA TOPOCHEMISTRY

One set of NIH 3T3 cells was fixed in a mixture of absolute ethanol–glacial acetic acid (3:1, v/v) for 1 min, rinsed in 70% ethanol, air dried at room temperature, and subjected to the Feulgen reaction with hydrolysis conducted in 4 M HCl for 60 min at 25°C. As a control for the 2 C ploidy degree, fixed mouse lymphocytes were subjected to the Feulgen reaction under hydrolysis conditions that permitted maximal depurination (4 M HCl for 90 min at 25°C). Another set of cells was fixed in 4% paraformaldehyde for 15 min, rinsed in phosphate saline buffer, air dried and subjected to immunocytochemistry to detect the HP1-α.

IMAGE ANALYSIS

False-colored images of Feulgen-stained NIH 3T3 cells were obtained with a Zeiss Axiophot 2 microscope and Kontron KS400-3 software (Oberkochen/Munich, Germany).

Images of the Feulgen-stained nuclei used for comparison of geometric, densitometric and textural parameters were obtained with a Zeiss automatic scanning microspectrophotometer (Carl Zeiss, Oberkochen, Germany) interfaced to a personal computer. The operating conditions used were the same as those previously reported for HeLa cells [Felisbino et al., 2011]. The cutoff point equal to absorbance 0.200 was selected to evaluate the areas covered by more condensed chromatin after a preliminary test was conducted for untreated controls and in comparison with previous reports [Mello and Russo, 1990]. One hundred nuclei were chosen at random and were measured individually for each experimental condition.

The image analysis parameters used were as follows: A_T, total integrated absorbance = nuclear Feulgen-DNA values or IOD (integrated optical density) in arbitrary units; A_C, integrated absorbance over the preselected cutoff ("condensed" chromatin Feulgen-DNA values); A_C %, "condensed" chromatin Feulgen-DNA

values relative to the nuclear (whole chromatin) Feulgen-DNA values; S_T, nuclear absorbing area in μm^2; S_C, area in μm^2 covered with stained chromatin showing absorbance above the selected cutoff point; S_C %, area covered with "condensed" chromatin relative to the nuclear area; and $AAR = (A_C/S_C)/(A_T/S_T)$, average absorption ratio, a dimensionless parameter that expresses how many times the average absorbance of the "condensed" chromatin exceeds that of the entire nucleus [Vidal et al., 2014]. A scatter diagram relating AAR to S_C % was plotted, as previously proposed [Vidal, 1984; Vidal et al., 2014] to permit the discrimination of the position of the points that correspond to specific nuclear phenotypes.

HDAC ASSAY

The enzymatic activity of HDACs in VPA- and TSA-treated cells expressed relative to the activity in the untreated controls was detected with an HDAC assay kit (Sigma®), following the manufacturer's instructions.

WESTERN BLOTTING

After the cells were treated with different concentrations of VPA and TSA, acetylated histone H3 was detected by Western blotting. These cells were then lysed by centrifugation in a buffer containing 30% glycerol, 1 mM PMSF, and 2 mM DTT, and their protein levels were measured using the Bradford method. Equal amounts of protein were separated by 17% SDS–PAGE and transferred onto nitrocellulose membranes (Applied Biosystem®, Carlsbad). The membranes were incubated in the blocking solution for 2 h at room temperature and with a monoclonal anti-H3 acetyl antibody (Millipore®, Billerica) overnight at 4°C, followed by extensive washing with TRIS-buffered saline-1% Triton X-100 (TBST). After that, the corresponding horseradish peroxidase-conjugated secondary antibody was added. The immunoreactive proteins were determined using an ECL Western blotting detection system (Amersham®, Pittsburgh, USA). Glyceraldehyde 3-phosphate dehydrogenase (GAPDH) was the loading control for histone H3 acetylation. Assays were repeated five times. Image J software (NIH, Bethesda) was used for the estimation of the acetylated H3 (H3ac)/GAPDH ratio.

IMMUNOCYTOCHEMISTRY

The spatial localization of HP1-α was investigated in the cells washed in PBS, incubated for 10 min in 3% hydrogen peroxide diluted in methanol, treated for 1 h in 1.5% blocking serum (Santa Cruz Biotech®, Santa Cruz) in PBS and incubated overnight in primary antibody (Cell Signaling Tech., Danvers, USA) at 4°C. A biotinylated anti-rabbit secondary antibody (Santa Cruz Biotech®) and an avidin–biotin enzyme reagent (Santa Cruz Biotech®) were used for the detection of HP1-α through diaminobenzidine (DAB) precipitation (Sigma®). The preparations were counterstained with methyl green.

MITOTIC ABNORMALITIES, MICRONUCLEATION, MITOTIC INDICES, AND CELL DEATH

The number of abnormal mitosis-containing lagging chromosomes, chromosome bridging and triple-polar spindles and the number of giant nuclei, micronuclei, mitotic indices and apoptotic ratios were estimated for all cases in the Feulgen-stained cells. Presence of extremely condensed chromatin or apoptotic bodies and mitotic catastrophe-like cell death characteristics were also investigated. Approximately 2,000 cells were examined per preparation.

QUANTITATIVE REAL-TIME RT-PCR

Total RNA was isolated from cells treated for 1 and 48 h with 1.0 and 5.0 mM VPA using the RNeasy Mini Kit (Qiagen®, Valencia). RNA was reverse transcribed using the High-Capacity cDNA Reverse Transcription Kit (Applied Biosystems®). RT-PCR was performed using an Applied Biosystems 7500 Real Time PCR system following standard protocols and TaqMan Gene Expression assays (Applied Biosystems®) for *CCND2* (Mm00432051_m1), *Bcl-2* (Mm00477631_m1), and *Bax* (Mm00432051_m1). Cycle threshold (Ct) values were calculated from experiments performed in triplicate and normalized with respect to the housekeeping gene *GAPDH*.

STATISTICS

Calculations and statistical analyses were performed using Minitab 12™ software (State College, PA), and the Mann–Whitney test. $P < 0.05$ was the critical level used for rejection of the null hypothesis. Comparisons of the H3ac/GAPDH ratio, the expression of *CCND2*, *Bcl-2*, and *Bax* and of the *Bcl-2/Bax* ratio in VPA-treated versus control cells were performed using Student's *t*-test.

RESULTS

CHROMATIN REMODELING IS INDUCED IN VIABLE NIH 3T3 CELLS BY VPA AND TSA

No loss of viability was statistically demonstrated using the MTT assay for NIH 3T3 cells treated with VPA and TSA at the concentrations and times of treatment used for investigation of chromatin remodeling (Fig. 1). The apparently lower values observed in some of the conditions resulted from the inclusion of one sample with a low value out of 12 total samples for the calculation of the respective mean value, causing the drop of this value and increase in respective standard error.

Preliminary analysis of Feulgen-stained nuclei in NIH 3T3 cells revealed false-color images suggestive of chromatin unpackaging as induced by VPA and TSA (Fig. 2). Nuclear areas covered by more condensed chromatin packaging (depicted as green points), which were abundant in untreated controls, appeared reduced in size in the VPA- and TSA-treated cells.

The scatter diagrams used, which relate nuclear relative areas covered with condensed chromatin (S_C %) to the level of textural contrast between condensed and total chromatin (AAR) [Vidal, 1984; Vidal et al., 2014], indicated that a decrease in S_C % values occurred that was concomitant with an increase in AAR values under all the tested VPA and TSA treatment conditions. These scatter plots have been basically proposed to permit the discrimination of points which correspond to the phenotypic image of each nucleus under consideration, depending on its position in the diagram [Vidal, 1984]. Figure 3 depicts this type of observation for 0.5 mM VPA-treated cells, a finding that was repeatedly verified in the cells subjected to the other experimental conditions (Supplementary Fig. 1). Statistical comparison confirmed the visual observations from the scatter diagrams and indicated that global chromatin decondensation

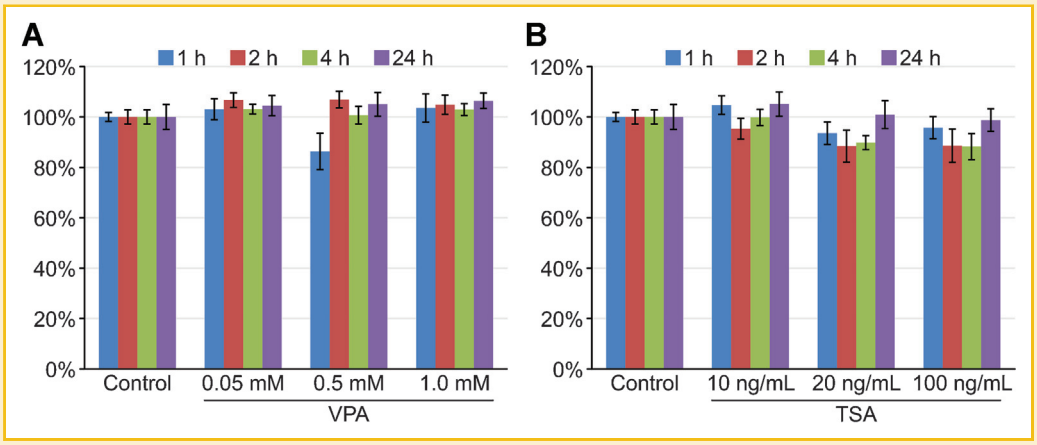

Fig. 1. Cell viability of VPA and TSA-treated NIH 3T3 cells as assessed with the MTT assay. No significant difference at $P_{0.05}$ occurred between VPA- (A) and TSA- (B) treated cells and the untreated controls.

occurred even during treatment of the NIH 3T3 cells at low VPA and TSA concentrations such as 0.05 mM and 10 ng/ml, respectively, and during periods as short as 1 h (Supplementary Table I).

With the objective of determining if chromatin decondensation induced by VPA and TSA affected euchromatin and areas covered with heterochromatin (Fig. 4), the number of nuclei with low S_C % (S_C % < 10%) after using a cutoff point equal to 0.200 with scanning microspectrophotometry [Mello and Russo, 1990], was determined in Feulgen-stained NIH 3T3 cells under the various experimental conditions. The percentage of nuclei with this S_C %, which in untreated cells varied from 0% to 1%, increased even after treatment with a low drug concentration (VPA, 24 h; TSA, short treatment period) or after a 24-h treatment period with ≥20 ng/ml TSA (Table I). These data indicate that the chromatin decondensation induced by both VPA and TSA also affects the heterochromatin areas in NIH 3T3 cells.

A significant increase in nuclear size occurred after all of the VPA treatments and in the majority of the TSA-treated cells (data not shown), which is in agreement with the proposition that these drugs induce chromatin decondensation in NIH 3T3 cells. This finding was reinforced by examining the relationship between nuclear areas and Feulgen-DNA amounts (integrated optical densities = IOD values) determined by microspectrophotometric image analysis (Supplementary Fig. 2).

CONCOMITANT TO CHROMATIN REMODELING, HDAC ACTIVITY, AND HISTONE H3 ACETYLATION ARE AFFECTED BY VPA AND TSA

A significant decrease in HDAC activity and increased acetyl histone H3 levels (detected with Western blotting for whole chromatin) were demonstrated in VPA- and TSA-treated cells when compared with untreated controls (Fig. 5A–D). This finding occurred under the same experimental conditions that demonstrated the induction of chromatin remodeling.

VPA AND TSA INDUCE HP1-α DISRUPTION FROM PERICENTRIC HETEROCHROMATIN

As expected because a mouse cell lineage was used, HP1-α was identified at the various condensed chromatin bodies that

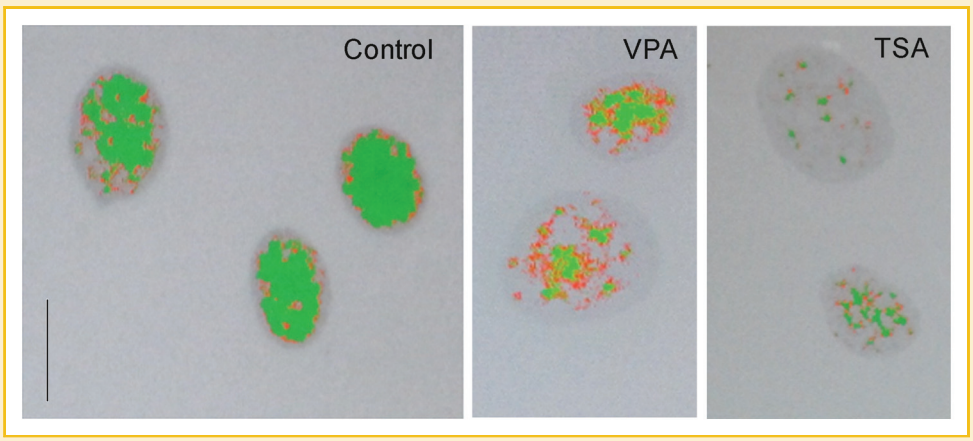

Fig. 2. False-colored images of Feulgen-stained, VPA- and TSA-treated NIH 3T3 cells. Condensed chromatin packaging revealed as green points covers smaller areas in VPA- and TSA-treated cells when compared to untreated control. Scale bar, 25 μm.

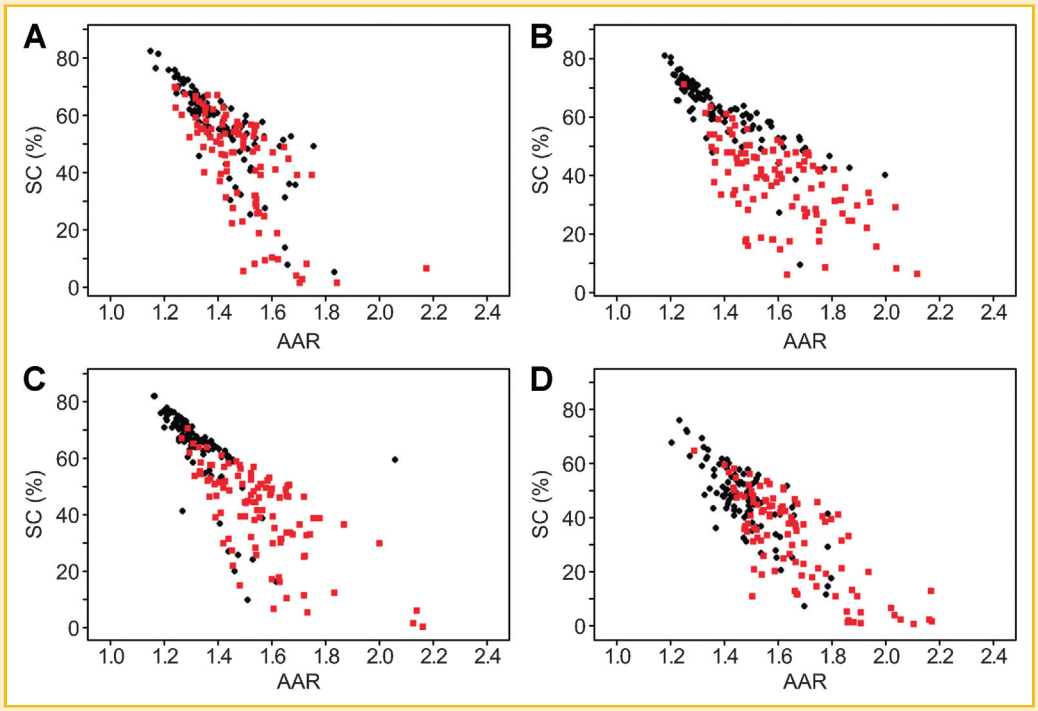

Fig. 3. Scatter diagrams of S_C % versus AAR for Feulgen-stained NIH 3T3 cells. A decrease in S_C % values concomitant with an increase in AAR values is observed for nuclei from cells treated with 0.5 mM VPA for 1 (A), 2 (B), 4 (C), or 24 h (D) (red square dots) in comparison with untreated controls (black dots); n, 100.

correspond to pericentric heterochromatin in the chromocenters [Maison et al., 2002] of untreated NIH 3T3 cells (Fig. 6A). In VPA- and TSA-treated cells the marks corresponding to HP1-α were no longer visible in most interphase cell nuclei (Figs. 6B and C).

CELL PROLIFERATION AND MICRONUCLEATION CHANGES REQUIRE DRASTIC VPA AND TSA TREATMENTS

Despite disruption of HP1-α from the chromocenter heterochromatin and that chromatin decondensation affected heterochromatin in the interphase nuclei under the various treatments with VPA and TSA, these phenomena were not sufficient to reduce the mitotic indices and to increase the frequency of micronuclei in NIH 3T3 cells, except under high concentrations of the HDACIs for 48 h (Table II). The expression of the *CCND2* gene, the product of which is required for the cell cycle G1/S transition, was not affected by VPA treatments (Fig. 7A). The frequency of mitotic cells containing chromosome bridges and lagging chromosomes, giant nuclei and nuclear buddings, abnormalities present in the NIH 3T3 cells under all of the experimental conditions used was not found to be significantly affected by longer treatments with high VPA and TSA concentrations (data not shown). An effect at this level possibly required a more extensive long-term treatment with higher concentrations of these HDACIs.

CELL DEATH IS NOT INDUCED EVEN WITH A DRASTIC VPA TREATMENT

The expression of the *Bcl-2* and *Bax* genes was increased after a treatment with 5.0 mM VPA for 48 h (Figs. 7B and C). However, the *Bcl-2/Bax* ratio was not affected with this treatment (Fig. 7D). In addition, a significant increase in the morphologically evaluated apoptotic ratios and in the frequency of cell death preceded by multinucleation following VPA and TSA treatments was not demonstrated (data not shown).

DISCUSSION

Present image analysis results indicate that VPA- and TSA-induced chromatin textural remodeling, that has been previously reported for tumor cells [Tóth et al., 2004; Rao et al., 2007; Felisbino et al., 2011], also occurs in non-transformed NIH 3T3 cells. These cells are an important model system used in a multitude of different investigations, including cell transformation [Mello and Russo, 1990; Ailenberg and Silverman, 2003; Leibiger et al., 2013]. The chromatin textural alterations in the NIH 3T3 cells at all VPA and TSA treatment conditions, that were not due to cytotoxicity effects, occurred simultaneously with decreased HDAC activity, as expected based on the activity of these HDACIs [Yoshida et al., 1995; Göttlicher et al., 2001; Phiel et al., 2001; Eyal et al., 2004; Rao et al., 2007; Kortenhorst et al., 2009]. These alterations were accompanied by a general increase in the degree of histone H3 acetylation. The effect of increasing total histone H3 acetylation was detected even at VPA and TSA concentrations lower than the concentrations reported for other cell types, including Swiss 3T3 cells [Gotfryd et al., 2010; Hezroni et al., 2011].

The chromatin remodeling induced in VPA- and TSA-treated NIH 3T3 cells also affected condensed chromatin areas identified as heterochromatin [Mello and Russo, 1990], in contrast to a reported

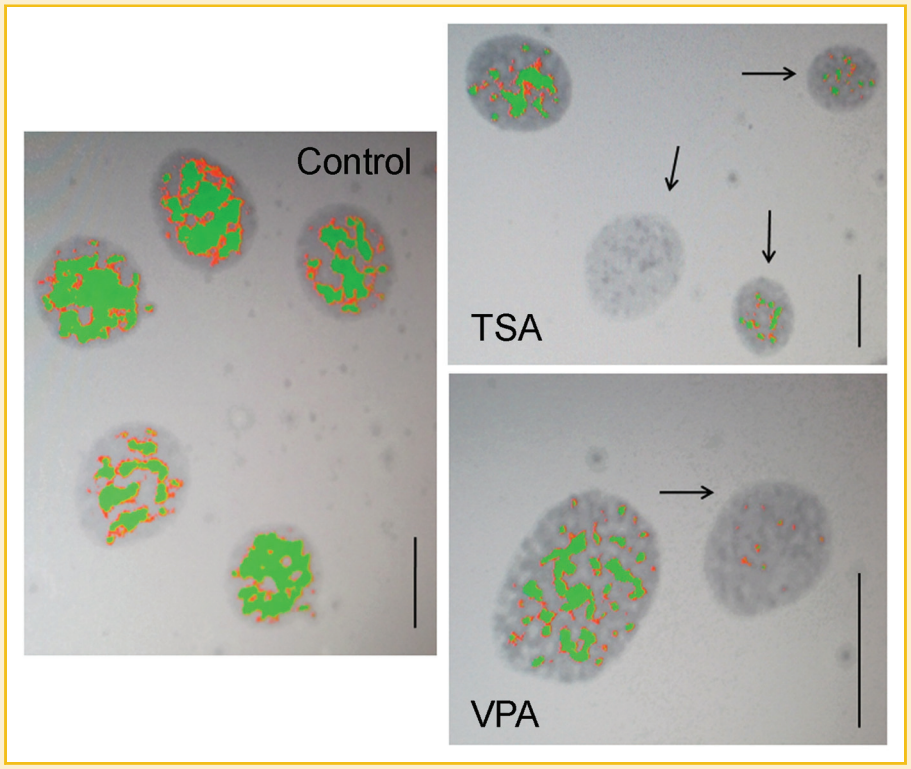

Fig. 4. Chromatin decondensation affecting heterochromatin areas in VPA- and TSA-treated NIH 3T3 cells. Arrows indicate Feulgen-stained nuclei in which the area covered with condensed chromatin (false-colored green points) is lower than 10% of the total nuclear area. Cells with less than 10% condensed chromatin appear with increased frequency after treatment for 24 h with 100 ng/ml TSA and 0.05 mM VPA, when compared with an untreated control. Scale bar, 25 μm.

disparity of histone deacetylase inhibition on the repair of radiation-induced DNA damage between euchromatic and heterochromatic compartments in K562 cells treated with these drugs [Karagiannis et al., 2007; Harikrishnan et al., 2008]. The heterochromatin areas affected by VPA and TSA in mouse somatic cells constitute chromocenters [Cerda et al., 1999]. A similar effect on heterochromatin unpackaging as promoted by VPA has been observed in another cell system, the polyploid cells of the insect *Triatoma infestans* (Alvarenga EM—unpublished data), where extensive nuclear compartments contain constitutive heterochromatin [Alvarenga et al., 2011]. Additionally, TSA has been reported to promote the decondensation of condensed chromosome territories and the

TABLE I. Frequency of Nuclei With S_C % <10% in VPA- and TSA-Treated NIH 3T3 Cells Determined With Scanning Microspectrophotometry Using a Cutoff Point = 0.200

Treatment Time (h)	Drugs	Concentration	Nuclear frequency (%)	Treatment Time (h)	Drugs	Concentration	Nuclear frequency (%)
1	VPA/TSA	Zero	1	4	VPA/TSA	Zero	0
	VPA	0.05 mM	5		VPA	0.05 mM	4
		0.5 mM	6			0.5 mM	5
		1.0 mM	11			1.0 mM	0
	TSA	10 ng/ml	41		TSA	10 ng/ml	2
		20 ng/ml	13			20 ng/ml	2
		100 ng/ml	19			100 ng/ml	9
2	VPA/TSA	Zero	1	24	VPA/TSA	Zero	1
	VPA	0.05 mM	2		VPA	0.05 mM	29
		0.5 mM	4			0.5 mM	13
		1.0 mM	8			1.0 mM	14
	TSA	10 ng/ml	6		TSA	10 ng/ml	5
		20 ng/ml	11			20 ng/ml	19
		100 ng/ml	5			100 ng/ml	20

TSA, trichostatin A; VPA, valproic acid.

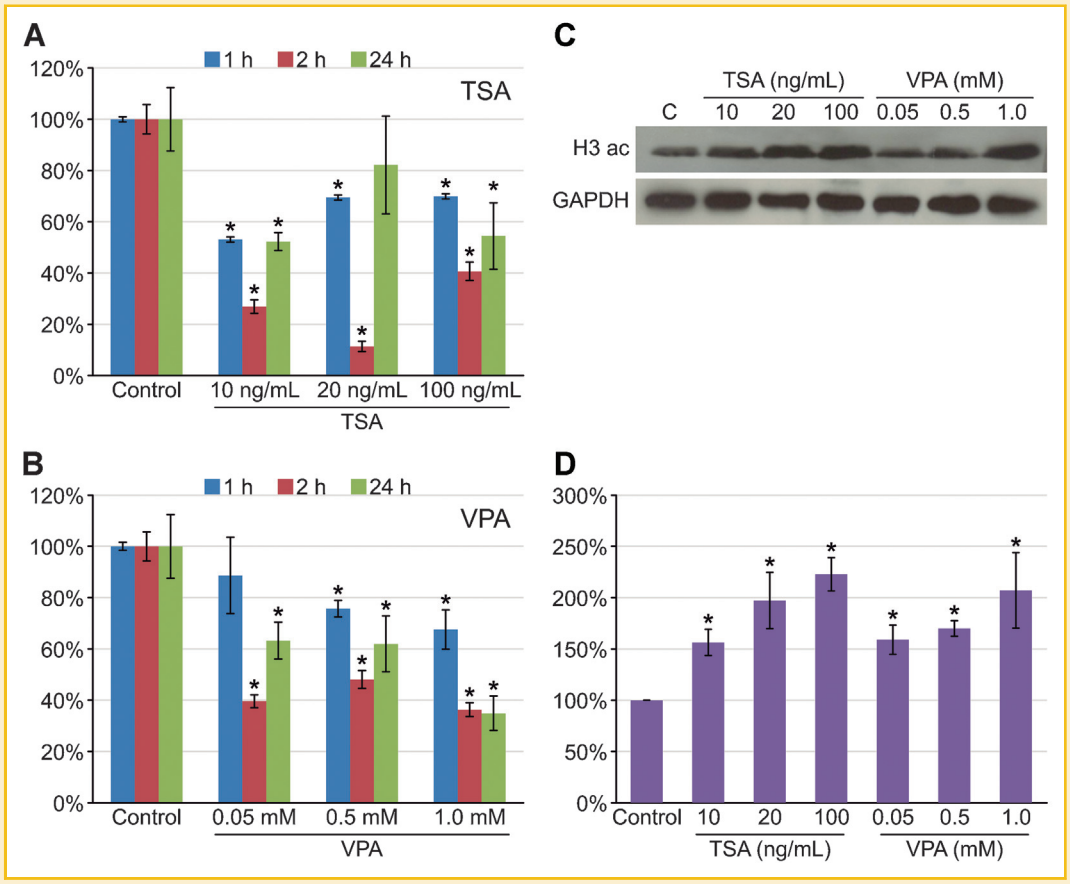

Fig. 5. Relative HDAC activity and the degree of H3 histone acetylation in NIH 3T3 cells. A significant decrease in HDAC activity in VPA- (A) and TSA-(B)-treated cells occurred in almost all treatment conditions when compared with the untreated controls. Western blotting analysis showed increased acetyl histone H3 levels in VPA- and TSA-treated cells, when compared with the untreated control (c) (C,D). GAPDH was the loading control for histone H3 acetylation. *Difference significant at $P_{0.05}$ in comparison to control (Student's *t*-test); n, 5.

reduction of heterochromatin content in lamin A/C-deficient fibroblasts [Galiová et al., 2008].

Moreover, in addition to causing the inhibition of histone deacetylases, VPA has been reported to induce the DNA demethylation of specific genes in certain cell types [Detich et al., 2003; Milutinovic et al., 2007]. The HDAC inhibition promoted by this drug and TSA has also been connected with increased H3K4 methylation [Harikrishnan et al., 2008] and decreased H3K9 methylation [Marinova et al., 2011]. All of these epigenetic alterations are known to affect chromatin condensation.

Although no record exists regarding HDACI-promoted histones or DNA demethylation in NIH 3T3 cells, decreased H3K9 methylation, in particular, may have contributed to the VPA- and TSA-induced chromatin remodeling observed in the heterochromatin areas of these cells. This hypothesis is supported by the present immunocytochemical results showing that HP1-α was depleted from the heterochromatic bodies of most NIH 3T3 cell nuclei by both VPA and TSA treatments, which has been considered as indicative of hypomethylation at histone H3K9me3 promoted by these HDACIs in several other systems [Bártová et al., 2008; Krebs et al., 2011]. The depletion of HP1-α in the present study is also in agreement with image analysis data showing that heterochromatin areas are unpacked following VPA and TSA treatments and with the findings obtained for MCF-7 cells, which indicate that non-histone proteins involved in determining chromatin structure are affected by HDACIs [Marchion et al., 2005]. Prolonged treatment of another mouse cell line (L929) with a low concentration of TSA has also been reported to cause at least a portion of their centromeric regions to cease binding HP1, even after TSA was removed from the cell culture [Taddei et al., 2001; Bártová et al., 2008].

The present findings regarding HP1-α depletion and chromatin decondensation in NIH 3T3 cell heterochromatin, as induced by VPA and TSA, do not necessarily implicate histone hyperacetylation at this chromatin territory. For example, in mouse embryonic stem cells treated with 0.5 mM VPA for 4 and 16 h, HDAC inhibition alone has been suggested to be insufficient to elevate the acetylation level of specific genomic regions; however, recruitment of histone acetyl transferases to these regions is required [Hezroni et al., 2011]. Particularly, in most genes with low initial acetylation levels in a condensed chromatin structure, there is no increase in the acetylation level after HDAC inhibition in these cells [Hezroni et al., 2011].

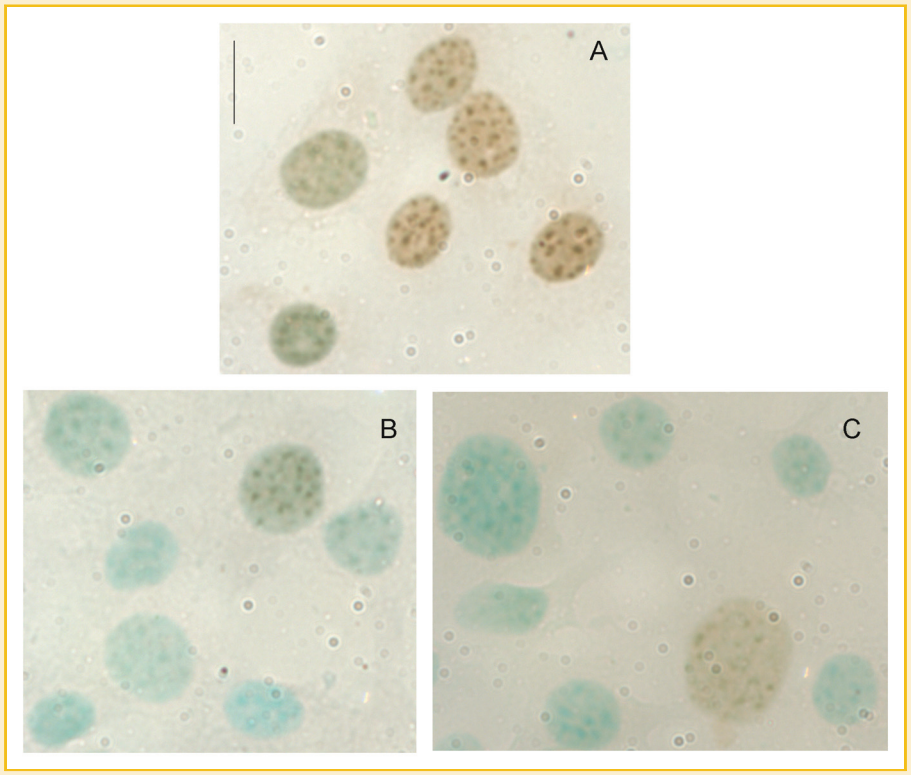

Fig. 6. Immunodetection of HP1-α in the heterochromatin of NIH 3T3 cells. Depletion of HP1-α is observed in VPA- (B) and TSA-(C) treated cells when compared with an untreated control (A). Scale bar, 25 μm.

The significant decrease in cell proliferation found only in NIH 3T3 cells treated with a high concentration of VPA and TSA is in agreement with findings in K562 cells [Harikrishnan et al., 2008]. The effect of the TSA treatment on the inhibition of cell proliferation in Balb/c 3T3 cells, similar to the silencing of HDAC3 expression, has been attributed to the hyperacetylation of H3K9 on the *gdf11* promoter, which would lead to the up-regulation of the *gdf11* gene and the simultaneous repression of the expression of the gene that encodes follistatin, a Gdf11 antagonist [Zhang et al., 2004]. The decreased cell proliferation in NIH 3T3 cells under high VPA concentrations for 48 h was not accompanied by alteration in the cyclin D2 gene expression, results that differed from those with VPA-treated HeLa and murine prostate cancer cells [Dejligbjerg et al., 2008; Witt et al., 2013]. In those cancer cell lines, the originally low *CCND2* expression becomes upregulated following VPA treatment [Dejligbjerg et al., 2008; Witt et al., 2013]. Considering that cyclin D2 functions at the G1/S transition of the cell cycle control system [Inaba et al., 1992; Meyyappan et al., 1998], a decrease in cell proliferation in treated NIH 3T3 cells most likely resulted from factors functioning at later stages of the cell cycle. In the human tumor cell lines MCF-7 and PC3, the effect of TSA on the arrest of the mitotic progression at prometaphase has been associated with the inefficiency of kinetochores to capture microtubules [Robbins et al., 2005]. HDAC3 deacetylase activity that is

TABLE II. Mitotic Index and Micronuclei in NIH 3T3 Cells Treated With VPA and TSA for 48 h and Stained With the Feulgen Reaction

Treatment		Mitotic index (%)			Micronuclei (%)			n
Drug	Concentration	X	S	Md	X	S	Md	
VPA	Zero	1.80	0.92	1.60[a]	1.98	0.41	1.90[a]	4
	5.0 mM	0.28	0.38	0.10[b]	2.94	0.86	2.70[b]	4
TSA	Zero	1.65	0.64	1.50[c]	1.65	0.30	1.60[c]	3
	100 ng/ml	0.20	0.08	0.20[d]	2.62	0.75	2.55[c]	3
	500 ng/ml	0.12	0.15	0.10[e]	3.15	0.34	3.20[d]	3

Md, median; n, number of preparations per experimental condition; S, standard deviation; TSA, trichostatin A; VPA, valproic acid; X, arithmetic mean. Total number of cells per experimental condition = 2,000. Superscript letters "a" and "b" in the Md columns of the mitotic index and of the micronuclei parameters indicate that the VPA group (b) differs significantly from respective control (a) at the $P_{0.05}$ level (Mann–Whitney test). Superscript letters "d" and "e" in the Md column of the mitotic index parameter and "d" in the Md column of the micronuclei parameter indicate that the TSA groups differ significantly from respective control (c) at the $P_{0.05}$ level (Mann–Whitney test).

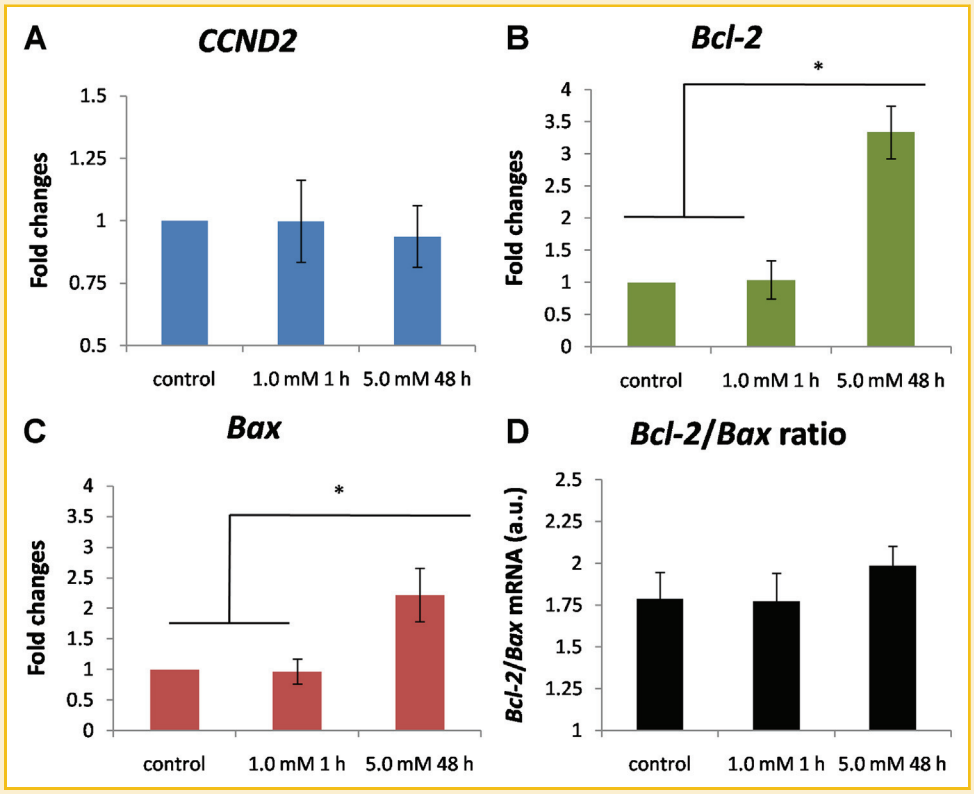

Fig. 7. *CCND2* (A), *Bcl-2* (B), and *Bax* (C) gene expression in VPA-treated NIH 3T3 cells. *CCND2* gene expression was not affected by VPA treatments (A). A significant increase in the expression of *Bcl-2* and *Bax* genes but no change in the *Bcl-2/Bax* ratio (D), is demonstrated for the cells treated with 5.0 mM VPA for 48 h. *Significant difference at $P_{0.05}$ (Student's *t*-test). Error bars indicate standard deviation of the mean. a.u., arbitrary units.

localized to the mitotic spindle, and is affected by ~200 ng/ml TSA, has recently been shown to be essential for spindle formation and chromosome alignment during mitosis in HeLa and mouse 3T3 cells [Ishii et al., 2008]. Potentially, VPA at high concentrations, which has been reported to inhibit microtubule formation [Cannell et al., 2002], may have exerted the same effect as TSA in affecting the spindle formation and decreasing cell proliferation in NIH 3T3 cells [Cannell et al., 2002; Ishii et al., 2008].

The increased number of micronuclei observed in NIH 3T3 cells under the same conditions that promoted the decrease in cell proliferation may have resulted from the inhibition of microtubule formation and the alteration of kinetochore assembly [Cannell et al., 2002]. The effect of TSA on micronucleus frequency at a concentration of 500 ng/ml in NIH 3T3 cells supports a previous report showing that 200 nM (~60.5 ng/ml) TSA induces significant levels of aneuploidy via nondisjunction events in human lymphoblasts in vitro [Olaharski et al., 2006]. This consequence, however, was not evident in NIH 3T3 cells in terms of the increase in mitotic abnormalities following VPA and TSA treatment.

The increased expression of *Bcl-2* and *Bax* genes with the 5.0 mM VPA treatment for 48 h is not sufficient to indicate an increase in caspase-3 activity and apoptosis in NIH 3T3 cells because the *Bcl-2/Bax* expression ratio and cell death ratios were not affected under this experimental condition [Oltvai et al., 1993; Basu and Haldar, 1998; Salakou et al., 2007]. Although HDACIs selectively induce apoptosis in cancer cells, the opposite effect has been described for non-cancer cells [Zhang et al., 2011]. Decreased caspase-3 levels have even been reported for TSA-treated 3T3 cells [Ailenberg and Silverman, 2003]. Considering that the increased expression of *Bcl-2* and *Bax* genes was verified for NIH 3T3 cells only under a treatment with a very high dose of VPA for 48 h, this event could not be associated with the presently described chromatin remodeling that was found to occur even under mild VPA treatments. Thus, it is important to reveal that VPA treatment does not affect cell death in non-tumoral fibroblastic cells such as NIH 3T3 cells, in contrast to the drug's known effect in tumor cells.

CONCLUSIONS

Even low doses of VPA and TSA applied for relatively short periods are capable of inducing chromatin remodeling in euchromatin and heterochromatin and promoting HP1-α depletion in non-transformed NIH 3T3 cells. The inhibition of HDACs by VPA and TSA as found in the present study does not necessarily imply that an increase in acetylation levels occurs in all chromatin territories and indiscriminately all over the genome. In terms of gene responsiveness to HDAC inhibition after considering reports for other cell systems, it is probable that in NIH 3T3 cells some genes may be up-regulated while other genes may be down-regulated [Jergil et al.,

2009, 2011]. *Bcl-2* and *Bax* genes are up-regulated under high-dose VPA treatment for 48 h; however their opposing action does not promote altered *Bcl-2/Bax* and apoptotic ratios. The VPA-induced effect on the expression of *Bcl-2* and *Bax* genes, which was found under high-dose VPA treatment, could not be directly associated with the presently described chromatin remodeling that was revealed even under mild VPA treatment. Based on induced HP1-α depletion from heterochromatic areas shown in this report, it is assumed that histone demethylation affecting H3K9me3 could be induced in NIH 3T3 cells. Although HP1-α depletion occurs in pericentromeric heterochromatin of the majority of NIH 3T3 cells even under mild VPA and TSA treatments, this event apparently does not interfere with the integrity of the mitotic spindle to the point of affecting mitotic rates and micronucleation and of increasing chromosome abnormalities at such treatment conditions. Drastic effects on cell proliferation and micronucleation for this cell system require an exposure of at least 48 h to high doses of VPA and TSA and, at least for VPA treatment, the effects should not be associated with cyclin D2 gene expression.

Finally, the detection of changes in the genome-wide signatures of NIH 3T3 cells after treatment with VPA and TSA, which was not the objective of the present work, is certainly relevant as a matter for further investigation. Most likely, genome-wide studies could reveal alterations in epigenetic markers more properly associated with gene expression and structural changes in the chromatin architecture promoted by these drugs. Such studies could shed insight into the changes introduced by these drugs regarding the expression of genes other than *CCND2*, *Bcl-2*, and *Bax* and reveal the temporal activation of particular metabolic pathways as investigated by others using mouse embryonic stem cells [Hezroni et al., 2011; Jergil et al., 2011]. These studies could also be extended to *ras*-transformed cells NIH 3T3 cells.

ACKNOWLEDGMENTS

We thank Dr. Liana Verinaud (Institute of Biology, Unicamp) for generously allowing the use of the ELISA reader (VersaMax™, Sunnyvale), Ana Lúcia Soledade for cell culture technical assistance and Camila D. L. Santos for assistance with cell counting. We also thank Dr. H.F. Carvalho (Institute of Biology, Unicamp) and the Laboratory of Multiuser Equipments (Medical School, Unicamp) for the availability of their real-time PCR equipment. This work was supported by the São Paulo State Research Foundation (FAPESP) and the Brazilian National Council for Research and Development (CNPq). The funders had no role in study design, data collection and analysis, decision to publish, or preparation of the manuscript.

REFERENCES

Ailenberg M, Silverman M. 2003. Differential effects of trichostatin A on gelatinase A expression in 3T3 fibroblasts and HT-1080 fibrosarcoma cells: implications for use of TSA in cancer therapy. Biochem Biophys Res Commun 302:181–185.

Alvarenga EM, Mondin M, Martins JA, Rodrigues VL, Vidal BC, Rincones J, Carazzolle MF, Andrade LM, Mello ML. 2011. Spatial distribution of AT- and GC-rich DNA within interphase cell nuclei of *Triatoma infestans* Klug. Micron 42:568–578.

Bártová E, Krejci J, Harnicarová A, Galiová G, Kozubek S. 2008. Histone modifications and nuclear architecture: A review. J Histochem Cytochem 56:711–721.

Basu A, Haldar S. 1998. The relationship between BcI2, Bax and p53: Consequences for cell cycle progression and cell death. Mol Hum Reprod 4:1099–1109.

Cannell GR, Bailey MJ, Dickinson RG. 2002. Inhibition of tubulin assembly and covalent binding to microtubular protein by valproic acid glucuronide *in vitro*. Life Sci 71:2633–2643.

Cerda MC, Berrios S, Fernandez-Donoso R, Garcyna S, Redi C. 1999. Organisation of complex nuclear domains in somatic mouse cells. Biol Cell 91:55–65.

Dejligbjerg M, Grauslund M, Litman T, Collins L, Qian X, Jeffers M, Lichenstein H, Jensen PB, Sehested M. 2008. Differential effects of class I isoform histone deacetylase depletion and enzymatic inhibition by belinostat or valproic acid in HeLa cells. Mol Cancer 7:70.

Denizot F, Lang R. 1986. Rapid colorimetric assay for cell growth and survival. Modifications to the tetrazolium dye procedure giving improved sensitivity and reliability. J Immunol Methods 89:271–277.

Detich N, Bovenzi V, Szyf M. 2003. Valproate induces replication-independent active DNA demethylation. J Biol Chem 278:27586–27592.

Duenas-Gonzalez A, Candelaria M, Perez-Plascencia C, Perez-Cardenas E, de la Cruz-Hernandes E, Herrera LA. 2008. Valproic acid as epigenetic cancer drug: Preclinical, clinical and transcriptional effects on solid tumors. Cancer Treat Rev 34:206–222.

Eyal S, Yagen B, Sobol E, Altschuler Y, Shmuel M, Bialer M. 2004. The activity of anti-epileptic drugs as histone deacetylase inhibitors. Epilepsia 45:737–744.

Felisbino MB, Gatti MSV, Veronezi GMB, Tamashiro WMSC, Mello MLS. 2013. Chromatin remodeling induced by histone deacetylase inhibitors (HDACis) in HeLa, NIH 3T3 and HepG2 cells [abstract]. Epigenet Chromatin 6:s18.

Felisbino MB, Tamashiro WMSC, Mello MLS. 2011. Chromatin remodeling, cell proliferation and cell death in valproic acid-treated HeLa cells. PLoS ONE 6:e29144.

Galiová G, Bartova E, Raska I, Krejci J, Kozubek S. 2008. Chromatin changes induced by lamin A/C deficiency and the histone deacetylase inhibitor trichostatin A. Eur J Cell Biol 87:291–303.

Gotfryd K, Skladchikova G, Lepekhin EA, Berezin V, Bock E, Walmod PS. 2010. Cell-type specific anti-cancer properties of valproic acid: Independent effects on HDAC activity and Erk1/2 phosphorylation. BMC Cancer 10:383.

Göttlicher M, Minucci S, Zhu P, Kramer OH, Schimpf A, Giavara S, Sleeman JP, Lo Coco F, Nervi C, Pelicci PG, Heinzel T. 2001. Valproic acid defines a novel class of HDAC inhibitors inducing differentiation of transformed cells. EMBO J 20:6969–6978.

Harikrishnan KN, Karagiannis TC, Chow MZ, El-Osta A. 2008. Effect of valproic acid on radiation-induced DNA damage in euchromatic and heterochromatic compartments. Cell Cycle 7:468–476.

Hasan A, Mitchell A, Schneider A, Halene T, Akbarian S. 2013. Epigenetic dysregulation in schizophrenia: Molecular and clinical aspects of histone deacetylase inhibitors. Eur Arch Psych Clin Neurosci 263:273–284.

Hezroni H, Sailaja BC, Meshorer E. 2011. Pluripotency-related, valproic acid (VPA)-induced genome-wide histone H3 lysine 9 (H3K9) acetylation patterns in embryonic stem cells. J Biol Chem 286:35977–35988.

Inaba T, Matsushime H, Valentine M, Roussel MF, Sherr CJ, Look AT. 1992. Genomic organization, chromosomal localization, and independent expression of human cyclin D genes. Genomics 13:565–574.

Ishii S, Kurasawa Y, Wong J, Yu-Lee LY. 2008. Histone deacetylase 3 localizes to the mitotic spindle and is required for kinetochore-microtubule attachment. Proc Natl Acad Sci USA 105:4179–4184.

Jergil M, Kultima K, Gustafson AL, Dencker L, Stigson M. 2009. Valproic acid-induced deregulation *in vitro* of genes associated *in vivo* with neural tube defects. Toxicol Sci 108:132–148.

Jergil M, Forsberg M, Salter H, Stockling K, Gustafson AL, Dencker L, Stigson M. 2011. Short-time gene expression response to valproic acid and valproic acid analogs in mouse embryonic stem cells. Toxicol Sci 121: 328–342.

Karagiannis TC, Harikrishnan KN, El-Osta A. 2007. Disparity of histone deacetylase inhibition on repair of radiation-induced DNA damage on euchromatin and constitutive heterochromatin compartments. Oncogene 26:3963–3971.

Kortenhorst MS, Isharwal S, van Diest PJ, Chowdhury WH, Marlow C, Carducci MA, Rodriguez R, Veltri RW. 2009. Valproic acid causes dose- and time-dependent changes in nuclear structure in prostate cancer cells in vitro and in vivo. Mol Cancer Ther 8:802–808.

Krebs JE, Goldstein ES, Kilpatrick ST. 2011. Lewin′s Genes X. Sudbury: Jones and Bartlett Publ. p. 930.

Leibiger C, Kosyakova N, Mkrtchyan H, Glei M, Trifonov V, Liehr T. 2013. First molecular cytogenetic high resolution characterization of the NIH 3T3 cell line by murine multicolor banding. J Histochem Cytochem 61:306–312.

Maison C, Bailly D, Peters AH, Quivy JP, Roche D, Taddei A, Lachner M, Jenuwein T, Almouzni G. 2002. Higher-order structure in pericentric heterochromatin involves a distinct pattern of histone modification and an RNA component. Nat Genet 30:329–334.

Marchion DC, Bicaku E, Daud AI, Sullivan DM, Munster PN. 2005. Valproic acid alters chromatin structure by regulation of chromatin modulation proteins. Cancer Res 59:3815–3822.

Marinova Z, Leng Y, Leeds P, Chuang DM. 2011. Histone deacetylase inhibition alters histone methylation associated with heat shock protein 70 promoter modifications in astrocytes and neurons. Neuropharmacol 60:1109–1115.

Mello MLS, Russo J. 1990. Image analysis of Feulgen-stained c-H-*ras*-transformed NIH/3T3 cells. Biochem Cell Biol 68:1026–1031.

Meyyappan M, Wong H, Hull C, Riabowol K. 1998. Increased expression of cyclin D2 during multiple states of growth arrest in primary and established cells. Mol Cell Biol 18:3163–3172.

Milutinovic S, D′Alessio AC, Detich N, Szyf M. 2007. Valproate induces widespread epigenetic reprogramming which involves demethylation of specific genes. Carcinogenesis 28:560–571.

Olaharski AJ, Ji Z, Woo JY, Lim S, Hubbard AE, Zhang L, Smith MT. 2006. The histone deacetylase inhibitor trichostatin A has genotoxic effects in human lymphoblasts *in vitro*. Toxicol Sci 93:341–347.

Oltvai ZN, Milkman CL, Korsmeyer SJ. 1993. Bcl-2 heterodimerizes in vivo with a conserved homolog, Bax, that accelerates programmed cell death. Cell 74:609–619.

Phiel CJ, Zhang F, Huang EY, Guenther MG, Lazar MA, Klein PS. 2001. Histone deacetylase is a direct target of valproic acid, a potent anticonvulsant, mood stabilizer, and teratogene. J Biol Chem 276:36734–36741.

Poplineau M, Doliwa C, Schnekenburger M, Antonicelli F, Diedrich M, Trussardi-Régnier A, Dufer J. 2013. Epigenetically induced changes in nuclear patterns and gelatinase expression in human fibrosarcoma cells. Cell Prolif 46:127–136.

Rao J, Bhattacharya D, Banerjee B, Sarin A, Shivashankar GV. 2007. Trichostatin-A induces differential changes in histone protein dynamics and expression in HeLa cells. Biochem Biophys Res Commun 363:263–268.

Robbins AR, Jablonski SA, Yen TJ, Yoda K, Robey R, Bates SE, Sackett DL. 2005. Inhibitors of histone deacetylases alter kinetochore assembly by disrupting pericentromeric heterochromatin. Cell Cycle 4:717–726.

Salakou S, Kardamakis D, Tsamandas AC, Zolota V, Apostolakis E, Tzelepi V, Papathanasopoulos P, Bonikos DS, Papapetropoulos T, Petsas T, Dougenis D. 2007. Increased Bax/Bcl-2 ratio up-regulates caspase-3 and increases apoptosis in the thymus of patients with myasthenia gravis. In Vivo 21:123–132.

Shoji M, Ninomiya I, Makino I, Kinoshita J, Nakamura K, Oyama K, Nakagawara H, Fujita H, Tajima H, Takamura H, Kitagawa H, Fushida S, Harada S, Fujimura T, Ohta T. 2012. Valproic acid, a histone deacetylase inhibitor, enhances radiosensitivity in esophageal squamous cell carcinoma. Int J Oncol 40:2140–2146.

Taddei A, Maison C, Roche D, Almouzni G. 2001. Reversible disruption of pericentric heterochromatin and centromere function by inhibiting deacetylases. Nat Cell Biol 3:114–120.

Taddei A, Roche D, Bickmore WA, Almouzni G. 2005. The effects of histone deacetylase inhibitors on heterochromatin: implications for anticancer therapy? EMBO Rep 6:520–524.

Tóth KF, Knoch TA, Wachsmuth M, Frank-Stöhr M, Stöhr M, Bacher CP, Müller G, Rippe K. 2004. Trichostatin A-induced histone acetylation causes decondensation of interphase chromatin. J Cell Sci 117:4277–4287.

Vidal BC. 1984. Polyploidy and nuclear phenotypes in salivary glands of the rat. Biol Cell 50:137–146.

Vidal BC, Felisbino MB, Mello ML. 2014. Image analysis of chromatin remodeling. In: Stockert JC, Espada J, Blázquez-Castro A, editors. Functional analysis of DNA and chromatin. Methods in molecular biology, v. 1094. New York: Springer Sci-Humana Press. pp 99–108.

Witt D, Burfeind P, von Hardenberg S, Opitz L, Salinas-Riester G, Bremmer F, Schweyer S, Thelen P, Neesen J, Kaulfuss S. 2013. Valproic acid inhibits the proliferation of cancer cells by re-expressing cyclin D2. Carcinogenesis 34:1115–1124.

Yoshida M, Horinouchi S, Beppu T. 1995. Trichostatin A and trapoxin: Novel chemical probes for the role of histone acetylation in chromatin structure and function. BioEssays 17:423–430.

Zhang X, Wharton W, Yuan Z, Tsai SC, Olashaw N, Seto E. 2004. Activation of the growth-differentiation factor 11 gene by the histone deacetylase (HDAC) inhibitor trichostatin A and repression by HDAC3. Mol Cell Biol 24:5106–5118.

Zhang Y, Yu G, Wang D, Hu Y, Lei W. 2011. ERK1/2 activation plays important roles in the opposite effects of Trichostatin A in non-cancer and cancer cells. Toxicon 5:932–937.

SUPPORTING INFORMATION

Additional supporting information may be found in the online version of this article at the publisher′s web-site.